High-p_T Higgs boson production at hadron colliders to $O(\alpha_s G_F^3)$

S. Mrenna*
Lauritsen Laboratory, California Institute of Technology, Pasadena, California 91125

C.-P. Yuan†
Department of Physics and Astronomy, Michigan State University, East Lansing, Michigan 48824
(Received 19 July 1995)

We study high-p_T Higgs boson production in hadron collisions at one loop to order $O(\alpha_s G_F^3)$. In particular, we investigate the process $g+q(\bar{q})\to q(\bar{q})+H$, where $q=u,d,c,s$, or b, for the CERN LHC (a $\sqrt{s}=14$ TeV proton-proton collider). Our results are compared to the $O(\alpha_s^3 G_F)$ and $O(\alpha_s G_F)$ calculations. The associated production of a high-p_T Higgs boson with a b quark or antiquark at $O(\alpha_s G_F^3)$ is comparable to the $O(\alpha_s^3 G_F)$ and $O(\alpha_s G_F)$ processes because of the large top quark mass and the additional contribution of electroweak gauge and Goldstone bosons. The associated production of light quarks, however, is not significant. We also comment on new physics effects in the framework of the electroweak chiral Lagrangian.

PACS number(s): 12.15.Lk, 14.80.Bn

I. INTRODUCTION

With the discovery of the top quark [1], the only remaining missing element of the standard model (SM) particle spectrum is the Higgs boson. Experimentally, there are only lower bounds on M_H. The CERN e^+e^- collider LEP I has placed the limit $M_H>64.5$ GeV [2]. Theoretically, there are upper bounds in the SM from unitarity and triviality arguments [3]. One goal of the future high energy physics experimental program is to discover the Higgs boson and verify its properties or determine the alternative mechanism of electroweak symmetry breaking. The search for the Higgs boson at LEP II is strictly limited by the available center of mass energy and luminosity, so that only $M_H<$ 90–95 GeV can be probed for an energy of 190 GeV and 500 pb^{-1} of data [4]. The reach of a high-luminosity Tevatron collider is better, but becomes challenging above $M_H=110$ GeV [5]. The CERN Large Hadron Collider (LHC), a proton-proton collider with $\sqrt{s}=14$ TeV, on the other hand, is hoped to have enough energy, luminosity, and instrumentation to decisively probe the energy scale associated with electroweak symmetry breaking. This task is not as straightforward as it may seem. One possible alternative to the SM is the minimal supersymmetric standard model (MSSM) with a constrained multidimensional parameter space [6]. The constrained MSSM models predict that the couplings of the lightest Higgs boson to SM particles is very SM-like, i.e., $\sin^2(\beta-\alpha)\simeq 1$, and its mass should be less than about 140 GeV [7]. In this case, to deduce supersymmetry, one must observe a superpartner directly or discern its presence in quantum corrections. Another alternative, a model with a strongly interacting scalar sector [8], predicts a greatly enhanced Higgs boson width even for a Higgs boson mass of a few hundred GeV, so that the Higgs boson signal can be hidden by backgrounds. Regardless of the scenario, a full verification of the properties of the Higgs boson requires a full theoretical understanding. In this investigation, we concentrate on the high-p_T production of Higgs bosons, which is sensitive to loop corrections. The $O(\alpha_s^3 G_F)$ contribution to high-p_T Higgs boson production was calculated previously [9], where $G_F=(\sqrt{2}v^2)^{-1}$ and the vacuum expectation value $v=$ 246 GeV. The associated production of the Higgs boson with two high-p_T gluons was also studied in the large m_t limit [10]. Here, we extend previous calculations to include the $O(\alpha_s G_F^3)$ contributions from electroweak gauge bosons, Goldstone bosons, and quarks at the one-loop level. In particular, since the top quark mass is large, we expect to see an enhancement in the associated production of a Higgs boson with a b quark or antiquark in some kinematic region. We also expect this channel to be sensitive to the coupling of the electroweak gauge bosons and Goldstone bosons to the Higgs boson, since its rate does not vanish in the limit that the $U(1)_Y$ and $SU(2)_L$ gauge couplings vanish.[1] We study this sensitivity in the framework of the electroweak chiral Lagrangian, which allows us to construct the most general effective Lagrangian that is consistent with $SU(2)_L\times U(1)_Y\to U(1)_{em}$ symmetry breaking. We show that with new physics, the $O(\alpha_s G_F^3)$ contribution can be comparable to the $O(\alpha_s^3 G_F)$ one-loop and $O(\alpha_s G_F)$ tree-level contributions for the association production of a high-p_T Higgs boson with a bottom quark or antiquark.

II. HIGH-p_T PRODUCTION OF THE HIGGS BOSON TO $O(\alpha_s G_F^3)$

To $O(\alpha_s G_F^3)$, the Higgs boson is produced at high p_T from quark-gluon, antiquark-gluon, and quark-antiquark ini-

*Present address: H.E.P. Theory Division, Argonne National Laboratory, Argonne, IL 60439; Electronic address: mrenna@hep.anl.gov

†Electronic address: yuan@msupa.pa.msu.edu

[1]The $O(\alpha_s^3 G_F)$ contribution does not depend on the electroweak gauge couplings, but is only sensitive to the coupling of the top quark to the Higgs boson.

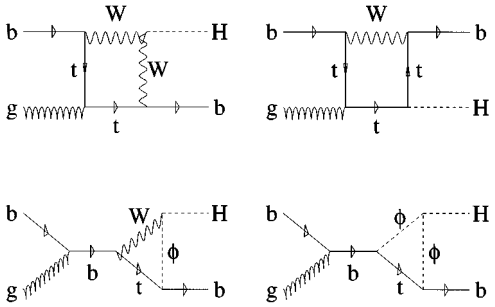

FIG. 1. Some representative Feynman diagrams for the $O(\alpha_s G_F^3)$ contributions to the process $g+b(\bar{b})\to b(\bar{b})+H$.

tial states. Since they are the most interesting, we will concentrate on the first two processes for the purpose of this discussion. The quark-antiquark annihilation process is typically an order of magnitude smaller at the LHC for $M_H \leqslant 400$ GeV. We shall perform the calculation in the helicity formalism, since the amount of algebra is reduced significantly. Furthermore, we shall use the Feynman rules in the 't Hooft–Feynman gauge, since the electroweak gauge bosons and their associated Goldstone bosons have equal masses and, hence, loop integrals involving gauge bosons and Goldstone bosons have the same denominators. This choice is also advantageous for investigating the electroweak chiral Lagrangian.

We consider the process $g(p_g)+q(p_j)\to q(p_i)+H(p_H)$ to $O(\alpha_s G_F^3)$, where the p_g and p_j are the four-momenta of the incoming particles and p_i and p_H are the four-momenta of the outgoing particles. The quark-antiquark initial state can be generated by the substitution $p_i\to -p_i, p_g\to -p_g$ and a reevaluation of the color factor. Contributions to the loop integral come from internal lines involving the weak isospin quark partner of q (we use the simplification $V_{ud}=V_{cs}=V_{tb}=1$), gauge bosons, and Goldstone bosons. Some representative Feynman diagrams are illustrated in Fig. 1. In this work, we have taken the limit $m_q\to 0$ for all q except t, unless stated otherwise. In the limit that $m_b\to 0$, there is no tree-level contribution from $g+b(\bar{b})\to b(\bar{b})+H$. Hence the result of the one-loop calculations considered here has to be finite after summing over the complete gauge invariant set of diagrams,[2] and a renormalization procedure is not needed. Furthermore, there is no contribution from either the γ-H or Z^0-H mixed self-energy diagram, because the amplitude vanishes when either the γ or Z^0 couples to a massless b (or $\bar{b}$) external leg due to the Ward identity. (Note that the two-point function γ-H or Z^0-H has to be proportional to the four-momentum of the γ or Z^0 due to Lorentz invariance.)

The amplitude for this process can be written as

$$\mathscr{M}_{\lambda_i\lambda_j\lambda_g} = ig_s\overline{u(\lambda_i,p_i)}[\mathscr{F}\gamma_\mu+\mathscr{G}_\mu \not{p}_H]u(\lambda_j,p_j)\epsilon^\mu_{\lambda_g}, \quad (1)$$

where λ_i and λ_j are the fermion helicity indices, λ_g is the gluon polarization, γ_μ are 4×4 γ matrices, $\not{a}=a^\mu\gamma_\mu$ for four-vector a^μ, and equations of motion have been applied to the on-shell, four-component spinors.

The complex scalar $\mathscr{F}$ and the complex vector $\mathscr{G}_\mu$ are form factors resulting from the integration of the loop momentum, and their explicit expressions are given in the Appendixes A and B. The helicity amplitude can be rewritten in terms of two-component Weyl spinors using the bra-ket notation:[3]

$$u_-(\lambda=-1/2,p_a)=\omega_+^a|p_a-\rangle,$$

$$v_-(\lambda=+1/2,p_a)=-\omega_+^a|p_a-\rangle,$$

$$u_+(\lambda=+1/2,p_a)=\omega_+^a|p_a+\rangle,$$

$$v_+(\lambda=-1/2,p_a)=-\omega_+^a|p_a+\rangle,$$

where $\omega_+^a=\sqrt{2E_a}$ for massless fermions with energy E_a, and $\langle p\pm|=(|p\pm\rangle)^\dagger$. These are the only components for massless fermions. For $p^\mu=E(1,s_\theta c_\phi,s_\theta s_\phi,c_\theta)$, where s_ψ and c_ψ are shorthand for $\sin\psi$ and $\cos\psi$ and E is the fermion energy,[4] $|p+\rangle=(\cos\theta/2,e^{i\phi}\sin\theta/2)^T$, and $|p-\rangle=(-e^{-i\phi}\sin\theta/2,\cos\theta/2)^T$. Also, the gluon polarization four-vectors for left-handed (L) and right-handed (R) helicities can be written as

$$\epsilon^\mu_{(L)}=\frac{e^{-i\phi}}{\sqrt{2}}[0,is_\phi+c_\phi c_\theta,-ic_\phi+s_\phi c_\theta,-s_\theta],$$

$$\epsilon^\mu_{(R)}=\frac{e^{i\phi}}{\sqrt{2}}[0,is_\phi-c_\phi c_\theta,-ic_\phi-s_\phi c_\theta,s_\theta],$$

where ϕ and θ are spherical coordinates of the gluon momentum. In the helicity basis, there are four nonvanishing amplitudes (as $m_q\to 0$). The parton-level cross section is

$$d\hat{\sigma}=\frac{1}{F}\frac{1}{S}C_{gb}\sum_{\lambda_g=L,R}(|\mathscr{M}_{--\lambda_g}|^2+|\mathscr{M}_{++\lambda_g}|^2)dR_2,$$

$$\mathscr{M}_{--\lambda_g}=ig_s\omega_+^i\omega_+^j\langle p_i-|[\mathscr{F}\gamma_{+\mu}+\mathscr{G}_\mu \not{p}_{H+}]|p_j-\rangle\epsilon^\mu_{\lambda_g},$$

$$\mathscr{M}_{++\lambda_g}=ig_s\omega_+^i\omega_+^j\langle p_i+|[\mathscr{F}\gamma_{-\mu}+\mathscr{G}_\mu \not{p}_{H-}]|p_j+\rangle\epsilon^\mu_{\lambda_g},$$

where the flux factor $F=2\hat{s}$ for $\hat{s}=(p_g+p_j)^2$; the spin average factor $S=2\times 2$; the color factor is $C_{gq}=4/(3\times 8)$ for $g+q\to q+H$, and $C_{q\bar{q}}=4/(3\times 3)$ for $q+\bar{q}\to g+H$; the gluon polarization is specified by λ_g; dR_2 is the two-body phase space; $\gamma^\mu_\pm$ are the 2×2 matrices $(\mathbf{1},\mp\sigma_i)$,[5] and $\not{a}_\pm=a_\mu\gamma^\mu_\pm$. In the above result, the amplitudes $\mathscr{M}_{++\lambda_g}$, which only contain contributions from Z^0 bosons, are small for two reasons. First, since we are only interested in initial

[2]The interference between the tree-level amplitude and the higher order amplitude is further suppressed by m_b because of their helicity structures.

[3]The two-component Weyl spinors are defined by the relation $u_\pm=\frac{1}{2}(1\pm\gamma_5)u$, etc.

[4]The superscript T denotes taking the transpose.

[5]σ_i are Pauli matrices satisfying $\mathrm{Tr}(\sigma_i\sigma_j)=2\delta_{ij}$.

and final states without t quarks, the internal quark is always light (because of the neutral current) and has a tiny coupling to the Goldstone boson.[6] Second, the left- and right-handed couplings of the Z^0 boson, which are smaller than the purely left-handed coupling of the $W^{\pm}$ bosons, appear in the squared matrix element to the fourth power. For all practical purposes, then, the Z^0 contributions can be ignored, leaving only two independent helicity amplitudes, $\mathscr{M}_{--\lambda_g}$, differing only in the gluon polarization.[7]

Because of gauge invariance, each amplitude satisfies the Ward identity resulting from replacing the gluon polarization vector with the gluon four-momentum. This simplifies to $\mathscr{F}+p_g\cdot\mathscr{G}=0$. The form factors are calculated numerically using the FF FORTRAN library [11], so the Ward identity can be verified numerically. Rotational and Lorentz invariance are also checked in the same manner.

The high-p_T production of the Higgs boson at a hadron collider is calculated by folding the parton-level cross section with the parton distribution functions (PDF's). We use CTEQ2L parton distribution functions [12] and choose both the factorization and the renormalization scales to be $\sqrt{\hat{s}}$. Unless otherwise stated, we use $m_t=175$ GeV in all calculations.

III. NUMERICAL RESULTS

In this section, we present results on high-p_T Higgs boson production at the LHC.[8] In Table I, we list the production cross section to $O(\alpha_s G_F^3)$, $O(\alpha_s^3 G_F)$, and $O(\alpha_s G_F)$, for several Higgs boson masses when the transverse momentum of the Higgs boson $p_T^H>50$ GeV. The tree-level $O(\alpha_s G_F)$ contribution is proportional to the square of the mass of the light quark and vanishes when the light quark mass is zero.[9] [In Appendix C, we show how to improve the tree-level calculation of the bH production rate to $O(\alpha_s^{(1,2)} G_F)$.] There are separate columns for the associated production of the Higgs boson with b quarks and u,d,s,c quarks (denoted by q). For all of these results, we include both the quark and antiquark contribution. For the associated production of H with a b quark or antiquark, the total $O(\alpha_s G_F^3)$ cross section for $p_T^H>50$ GeV is as large as $\sim 20\%$ of the $O(\alpha_s^3 G_F)$ cross section for $M_H=100-200$ GeV, and the $O(\alpha_s G_F)$ contribution is about the same as the $O(\alpha_s^3 G_F)$ contribution for $M_H<200$ GeV and is less important than the $O(\alpha_s G_F^3)$ contribution for $M_H>400$ GeV. For the $O(\alpha_s G_F^3)$ process, the m_t dependence is minimal. For example, when $M_H=110$ GeV, the total $O(\alpha_s G_F^3)$ cross section varies from 16.9 fb to 17.5 fb for $m_t=160$ GeV and 190 GeV, respectively. For the associated production of H with a light quark or antiquark, the $O(\alpha_s G_F^3)$ cross section for $p_T^H>50$ GeV is never more than about 2% of the $O(\alpha_s^3 G_F)$ cross section in the same M_H range. The cross section for $q+\bar{q}\to H+g$ is much smaller than that for the corresponding process $g+q(\bar{q})\to q(\bar{q})+H$, having values (1.5,0.15) fb for $M_H=$ (110,400) GeV, and will not be discussed further.

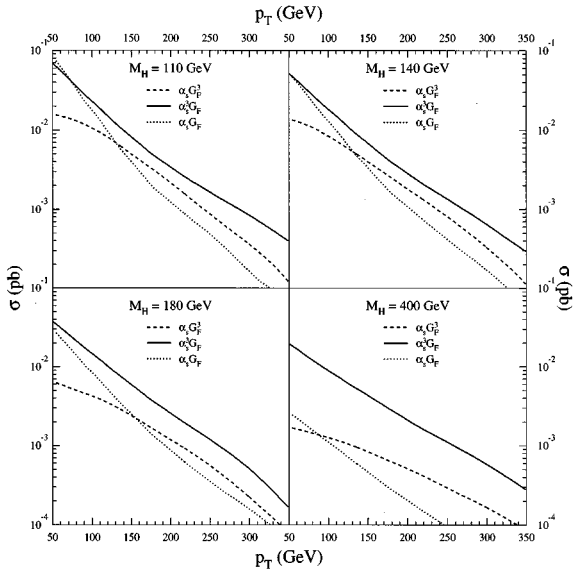

FIG. 2. The cross section integrated above p_T^H for $b(\bar{b})+H$ production to $O(\alpha_s G_F^3)$ and $O(\alpha_s^3 G_F)$ for various M_H.

It is interesting to note the relative sizes of the production rates. First, the one-loop $O(\alpha_s^3 G_F)$ rate is almost the same as the tree-level $O(\alpha_s G_F)$ rate, despite the usual $1/16\pi^2$ suppression from the loop process. This is because the gluon parton density is much larger than the quark parton density in the kinematic region to produce a Higgs boson with mass $\leqslant 400$ GeV at the LHC, and the constituent cross section of the tree-level process is proportional to m_b^2/v^2. Second, the one-loop $O(\alpha_s G_F^3)$ process is competitive with the one-loop $O(\alpha_s^3 G_F)$ process because of the large top quark mass in loop integrals. Finally, the $O(\alpha_s G_F)$ tree-level rates are not small despite the fact that they are proportional to the square of the b-quark (running) mass.

We also studied the p_T^H dependence of the cross section as a function of M_H. In Fig. 2, we show the cross section integrated above p_T^H for $b(\bar{b})+H$ production to $O(\alpha_s G_F^3)$, $O(\alpha_s^3 G_F)$, and $O(\alpha_s G_F)$, in the same M_H range as in Table I. The mean p_T^H, $\langle p_T^H\rangle$, of the $O(\alpha_s G_F^3)$ process, for p_T^H in the range of 50–350 GeV, is a slowly varying function of M_H below $M_H=180$ GeV, with a value of approximately

TABLE I. Cross section for Higgs boson production at high p_T.

Higgs boson production, $p_T^H>50$ GeV, $m_t=175$ GeV					
M_H	$\sigma[g+b(\bar{b})\to b(\bar{b})+H]$ (fb)			$\sigma[g+q(\bar{q})\to q(\bar{q})+H]$ (fb)	
(GeV)	$O(\alpha_s G_F^3)$	$O(\alpha_s^3 G_F)$	$O(\alpha_s G_F)$	$O(\alpha_s G_F^3)$	$O(\alpha_s^3 G_F)$
110	15.6	71.6	92.8	42.4	2.2×10^3
140	13.5	53.3	56.3	33.1	1.6×10^3
180	6.4	38.5	31.2	21.8	1.2×10^3
400	1.7	20.0	2.9	0.4	0.7×10^3

[6]This coupling vanishes for massless quark.

[7]In our numerical results, we include all the contributions.

[8]The rate at a 2 TeV ($\bar{p}p$) collider is about two orders of magnitude smaller than that at 14 TeV (pp) collider, and is too small to be observed for all practical purposes.

[9]We have used the running mass of the bottom quark for calculating the production rate of the tree-level process $g+b(\bar{b})\to b(\bar{b})+H$.

120 GeV. For $M_H=400$ GeV, $\langle p_T^H\rangle$ is 152 GeV. The $\langle p_T^H\rangle$ of the $O(\alpha_s^3 G_F)$ and $O(\alpha_s G_F)$ processes is strongly dependent on the lower transverse momentum cutoff needed to regulate the $p_T^H\to 0$ divergence associated with the gluon propagator, and is somewhat smaller than that for the $O(\alpha_s G_F^3)$ process.

In summary, we find that to accurately predict the cross section and test the properties of an intermediate mass Higgs boson produced at high p_T in association with b quarks and antiquarks, the $O(\alpha_s G_F^3)$ contributions should be included with the $O(\alpha_s^3 G_F)$ and $O(\alpha_s G_F)$ contributions. The production rate of $O(\alpha_s G_F^3)$ for the associated production of the Higgs boson with a light quark or antiquark is only a few percent of the $O(\alpha_s^3 G_F)$ rate, and probably is not distinguishable from the uncertainty in the theoretical calculations (e.g., PDF dependence).

IV. THE ELECTROWEAK CHIRAL LAGRANGIAN AND NONSTANDARD MODEL COUPLINGS

The process under consideration is sensitive to electroweak symmetry breaking in three different sets of couplings. First, there is the t-b-W vertex. The additional nonstandard couplings can be deduced from the chiral Lagrangian [13]

$$\mathscr{L}=-\sqrt{2}\kappa_L^{CC}\overline{t_L}\gamma^\mu b_L\Sigma_\mu^+-\sqrt{2}\kappa_L^{CC\dagger}\overline{b_L}\gamma^\mu t_L\Sigma_\mu^- -\sqrt{2}\kappa_R^{CC}\overline{t_R}\gamma^\mu b_R\Sigma_\mu^+-\sqrt{2}\kappa_R^{CC\dagger}\overline{b_R}\gamma^\mu t_R\Sigma_\mu^-, \quad (2)$$

where $\Sigma_\mu^\pm=1/\sqrt{2}\,(\Sigma_\mu^1\mp i\Sigma_\mu^2)$ for $\Sigma_\mu^a=-(i/2)\mathrm{Tr}(\sigma^a\Sigma^\dagger D_\mu\Sigma)$, and the action of the covariant derivative is $D_\mu\Sigma=\partial_\mu\Sigma-igW_\mu^a(\sigma^a/2)\Sigma+ig'\Sigma B_\mu(\sigma^3/2)$. The matrix field $\Sigma=\exp[i(\phi^a\sigma^a/v)]$, where $\sigma^a, a=1,2,3$, are the Pauli matrices, and ϕ^a's are the Goldstone bosons. Second, there is the Yukawa coupling between the Higgs boson and top quark. The most general Yukawa coupling of the fermion doublet F in the chiral Lagrangian is [13]

$$\mathscr{L}=-\frac{c_0}{v}H\bar{F}MF, \quad (3)$$

where M is a 2×2 mass matrix. In the standard model, $c_0=1$. Third, the coupling of the Higgs boson and the electroweak Goldstone bosons comes from the Lagrangian [13]

$$\mathscr{L}=\frac{1}{2}\partial_\mu H\partial^\mu H-\frac{1}{2}M_H^2H^2-V(H)+\left(\frac{c_1}{2}vH+\frac{c_2}{4}H^2\right)\mathrm{Tr}(D_\mu\Sigma^\dagger D^\mu\Sigma), \quad (4)$$

where $V(H)$ is the potential energy of the Higgs boson field. In the standard model, $c_1=c_2=1$.

To illustrate that new physics effects may enhance the $O(\alpha_s G_F^3)$ rate but not the $O(\alpha_s^3 G_F)$ or $O(\alpha_s G_F)$ rate, we study the effects of new physics arising from the scalar sector of the Lagrangian, as shown in Eq. (4). In this case, the $O(\alpha_s^3 G_F)$ and $O(\alpha_s G_F)$ contributions are not modified. As shown in Ref. [8], some models of the symmetry breaking sector allow the coefficient c_1 in Eq. (4) to be larger than 1. (c_2 is irrelevant to the processes of interest.) For instance, $c_1=\sqrt{8/3}$ was discussed in Ref. [8]. Because new physics can simultaneously modify the interactions of t-b-W and W-W-H, we do not intend to give predictions for any specific model. For simplicity, we only study the effects of new physics due to c_1 in the limit that the $\mathrm{SU}(2)_L\times\mathrm{U}(1)_Y$ gauge couplings g and g' vanish. Table II contains some of our results.

TABLE II. Effects of new physics on high-p_T Higgs boson production as $g,g'\to 0$. In the standard model, $c_1=1$.

	Higgs boson + $b(\bar{b})$ rate (fb) as $g,g'\to 0$ $p_T^H>30$ GeV, $m_t=175$ GeV				
M_H	Chiral Lagrangian coefficient c_1				
(GeV)	-0.5	0.0	0.5	1.0	1.5
110	1.09	0.87	0.78	0.83	1.01
140	1.26	0.79	0.87	1.49	2.64
180	0.74	0.69	2.00	4.67	8.71
200	0.42	0.63	1.76	3.82	6.81
250	0.19	0.49	1.32	2.70	4.60
300	0.12	0.36	1.00	2.01	3.41
400	0.06	0.21	0.59	1.20	2.03

Although these rates do not represent the true rates of the process $g+b(\bar{b})\to b(\bar{b})+H$ at the order $O(\alpha_s G_F^3)$,[10] they illustrate that the rates can vary by about a factor of 2 for a heavier Higgs boson. If the electroweak corrections to high-p_T Higgs boson production are substantially modified by new physics at the order $O(\alpha_s G_F^3)$, then this can be observed at future hadron colliders.

V. DISCUSSION AND CONCLUSIONS

Because the top quark mass is large and of the same order as v, the interaction of the top quark and the Goldstone bosons is strong and, therefore, can be sensitive to the electroweak symmetry-breaking sector. For the associated production of a b quark or antiquark with a Higgs boson at high p_T, the SM electroweak corrections of $O(\alpha_s G_F^3)$, involving the large top quark mass, is comparable to the one-loop $O(\alpha_s^3 G_F)$ and the tree-level $O(\alpha_s G_F)$ contributions (cf. Table I). On the other hand, the associated production of light quarks and antiquarks with the Higgs boson is not significant because no large fermion mass is involved.

Once the Higgs boson is discovered, it is important to test whether it is a standard model Higgs boson or some other nonstandard scalar particle. The cross section of the Higgs boson production at large transverse momentum can be sensitive to new physics which modify either t-b-W, t-t-H, or W-W-H vertices. Among them, only the t-t-H vertex can modify the $O(\alpha_s^3 G_F)$ contributions, while the $O(\alpha_s G_F)$ contribution is unchanged. In contrast, all of them can modify the $O(\alpha_s G_F^3)$ contributions. As illustrated in Table II, it is possible that the $O(\alpha_s G_F^3)$ rate is enhanced by more than a

[10] For $c_1=1$, i.e., in the SM, the $O(\alpha_s G_F^3)$ cross sections for $p_T^H>30$ GeV are (17.1,15.1,7.4,1.9) fb for $M_H=$ (110,140,180,400) GeV.

factor of 2 due to new physics effects. Therefore, $O(\alpha_s G_F^3)$ contributions should also be included when testing SM predictions for the production of the Higgs boson at hadron colliders.

ACKNOWLEDGMENTS

C.P.Y. thanks A. Abbasabadi, D. Bower-Chao, and W. Repko for useful discussions. S.M. was supported in part by DOE Grant No. DE-FG03-92-ER40701. The work of C.P.Y. was supported in part by NSF Grant No. PHY-9309902.

APPENDIX A: LOOP INTEGRATION

In calculating the helicity amplitudes, one must evaluate loop integrals of the form

$$X \equiv \frac{1}{i\pi^2}\int \frac{d^nQ\{1,Q^\mu,Q^\mu Q^\nu\}}{(Q^2-m_1^2)[(Q+P)^2-m_2^2]\cdots}.$$

For triangle diagrams, $X=C$, and for box diagrams, $X=D$.

Triangle diagrams

The scalar function for triangle diagrams, showing explicitly its dependent variables, is

$$C_0(m_1^2,m_2^2,m_3^2,p_1^2,p_2^2,p_3^2)=\frac{1}{i\pi^2}\int \frac{d^nQ}{(Q^2-m_1^2)[(Q+p_1)^2-m_2^2][(Q+p_1+p_2)^2-m_3^2]},$$

where the internal line masses m_i are labeled by the external lines, p_1 is the momentum flowing between the lines with masses m_1 and m_2, p_2 between m_2 and m_3, and $p_3=-p_1-p_2$ between m_3 and m_1. The vector integral over Q^μ is

$$C_{11}p_1^\mu + C_{12}p_2^\mu.$$

Similarly, the tensor integral over $Q^\mu Q^\nu$ is

$$C_{21}p_1^\mu p_1^\nu + C_{22}p_2^\mu p_2^\nu + C_{23}\{p_1^\mu p_2^\nu + p_1^\nu p_2^\mu\} + C_{24}g^{\mu\nu}.$$

Box diagrams

The scalar function for box diagrams, similar to the triangle diagrams, can be written as $D_0[m_1^2,m_2^2,m_3^2,m_4^2,p_1^2,p_2^2,p_3^2,p_4^2,(p_1+p_2)^2,(p_2+p_3)^2]$. The notation is an obvious generalization of that for the triangle diagrams. The vector integral over Q^μ is

$$D_{11}p_1^\mu + D_{12}p_2^\mu + D_{13}p_3^\mu.$$

The tensor integral over $Q^\mu Q^\nu$ is

$$D_{21}p_1^\mu p_1^\nu + D_{22}p_2^\mu p_2^\nu + D_{23}p_3^\mu p_3^\nu + D_{24}\{p_1^\mu p_2^\nu + p_1^\nu p_2^\mu\} + D_{25}\{p_1^\mu p_3^\nu + p_1^\nu p_3^\mu\} + D_{26}\{p_2^\mu p_3^\nu + p_2^\nu p_3^\mu\} + D_{27}g^{\mu\nu}.$$

APPENDIX B: FORM FACTORS

In 't Hooft–Feynman gauge, there are 20 Feynman diagrams containing $W^\pm$ bosons and $\phi^\pm$ Goldstone bosons involved in the process $g+b(\bar{b})\to b(\bar{b})+H$ at $O(\alpha_s G_F^3)$ for $m_b=0$. As discussed in the text, the three diagrams involving Z^0 bosons and ϕ^0 Goldstone bosons are negligible. Some typical diagrams are shown in Fig. 1. In this appendix, we list the individual contributions to the form factors [cf. Eq. (1)] from each Feynman diagram for the process $g(q_g)+b(q_3)\to b(q_1)+H(q_2)$. All momenta are defined pointing *in* to the Feynman diagram, i.e., the outgoing quark (q_1) and Higgs boson (q_2) four-momenta have a negative energy component. There are 12 triangle diagrams, with terms labeled $\mathscr{F}_9-\mathscr{F}_{20}$, and eight box diagrams, with terms $\mathscr{F}_1-\mathscr{F}_8$ and $\mathscr{G}_1^\mu-\mathscr{G}_8^\mu$. The full form factors are $\mathscr{F}=\Sigma_{i=1}^{20}\mathscr{F}_i$ and $\mathscr{G}^\mu=\Sigma_{i=1}^{8}\mathscr{G}_i^\mu$. The following expressions contain the invariant masses $s_{ij}=(q_i+q_j)^2$ and $s=(q_1+q_2+q_3)^2=q_g^2$. We have used the relation $M_W=\frac{1}{2}gv$ to reexpress the electroweak coupling constants in terms of masses and the vacuum expectation value v. The process involving light quarks in the initial and final state can be deduced by setting $m_t=0$. The limit $g,g'\to 0$, which we take to study the electroweak chiral Lagrangian, is obtained by eliminating all terms with an explicit M_W dependence. All triangle diagrams contain propagators for one fermion and two gauge or Goldstone bosons. The box diagrams fall into two categories, those containing two fermion and two gauge or Goldstone boson propagators (denoted t-t-W-W) and those containing three fermion and one gauge or Goldstone boson propagators (denoted t-t-t-W).

Triangle diagrams

$$\mathscr{F}_9 = -8C_{12}M_W^4/v^3,$$

$$\mathscr{F}_{10} = -2C_{12}m_t^2M_H^2/v^3,$$

$$\mathscr{F}_{11} = 2m_t^2M_W^2(-2C_0 - C_{12})/v^3,$$

$$\mathscr{F}_{12} = -2m_t^2M_W^2(-C_0 + C_{12})/v^3,$$

$$\mathscr{F}_{13} = -8C_{12}M_W^4/v^3,$$

$$\mathscr{F}_{14} = -2C_{12}m_t^2M_H^2/v^3,$$

$$\mathscr{F}_{15} = 2m_t^2M_W^2(C_0 - C_{12})/v^3,$$

$$\mathscr{F}_{16} = -2m_t^2M_W^2(2C_0 + C_{12})/v^3,$$

$$\mathscr{F}_{17} = 2m_t^2M_W^2(-2C_0 - 4C_{11})/v^3,$$

$$\mathscr{F}_{18} = 2m_t^4(-C_0 - 2C_{11})/v^3,$$

$$\mathscr{F}_{19} = 2m_t^2M_W^2(-2C_0 - 4C_{11})/v^3,$$

$$\mathscr{F}_{20} = 2m_t^4(-C_0 - 2C_{11})/v^3.$$

Note that there are no tensor contributions from the triangle diagrams, i.e., no C_{2i}.

Box diagrams

t-t-W-W diagrams:

$$\mathscr{F}_1 = -8M_W^4[2D_{27} - D_0m_t^2 + (D_{22} - D_{24} + D_{25} - D_{26})M_H^2 + (D_{11} + D_{25})s + (D_{24} - D_{25})s_{12} - (D_{11} + D_{12} - D_{25} + D_{26})s_{23}]/v^3,$$

$$\mathscr{F}_2 = -2m_t^2M_H^2[2D_{27} - D_0m_t^2 + (D_{22} - D_{24} + D_{25} - D_{26})M_H^2 + (D_{13} + D_{25})s + (D_{12} - D_{13} + D_{24} - D_{25})s_{12} - (D_{25} - D_{26})s_{23}]/v^3,$$

$$\mathscr{F}_3 = -2m_t^2M_W^2[-2D_{27} + D_{13}s + (2D_0 + D_{12} - D_{13})s_{12}]/v^3,$$

$$\mathscr{F}_4 = 2m_t^2M_W^2[2D_{27} + (D_0 + D_{11})s + (-2D_0 - D_{11} + D_{12})s_{23}]/v^3,$$

$$\mathscr{G}_1^\mu = -16M_W^4[(-D_{11} - D_{24})q_1^\mu + (-D_{12} - D_{22})q_2^\mu + (-D_{12} - D_{26})q_3^\mu]/v^3,$$

$$\mathscr{G}_2^\mu = -4m_t^2M_H^2[(-D_{12} - D_{24})q_1^\mu + (-D_{12} - D_{22})q_2^\mu + (-D_{13} - D_{26})q_3^\mu]/v^3,$$

$$\mathscr{G}_3^\mu = -4m_t^2M_W^2[(-2D_0 - 2D_{11} - D_{12} - D_{24})q_1^\mu + (-2D_0 - 3D_{12} - D_{22})q_2^\mu + (-3D_{13} - D_{26})q_3^\mu]/v^3,$$

$$\mathscr{G}_4^\mu = 4m_t^2M_W^2[(-2D_0 - 2D_{11} + D_{12} + D_{24})q_1^\mu + (-D_{12} + D_{22})q_2^\mu + (-D_{13} + D_{26})q_3^\mu]/v^3.$$

t-t-t-W diagrams:

$$\mathscr{F}_5 = 4m_t^2M_W^2[D_0m_t^2 + (-D_{22} + D_{24} - D_{25} + D_{26})M_H^2 - (2D_{11} + D_{25})s + (-D_{24} + D_{25})s_{12} + (-D_0 + 2D_{11} - 2D_{12} + D_{25} - D_{26})s_{23}]/v^3,$$

$$\mathscr{F}_6 = 2m_t^4[D_0m_t^2 + (-D_{22} + D_{24} - D_{25} + D_{26})M_H^2 - (2D_{13}s + D_{25})s + (-D_0 - 2D_{12} + 2D_{13} - D_{24} + D_{25})s_{12} + (D_{25} - D_{26})s_{23}]/v^3,$$

$$\mathscr{F}_7 = 4m_t^2M_W^2[D_0m_t^2 + (-D_{22} + D_{24} - D_{25} + D_{26})M_H^2 + (D_0 - D_{11} + D_{13} - D_{25})s + (-D_0 + D_{12} - D_{13} - D_{24} + D_{25})s_{12} + (D_{11} - D_{12} + D_{25} - D_{26})s_{23}]/v^3,$$

$$\mathscr{F}_8 = 2m_t^4[D_0m_t^2 + (-D_{22} + D_{24} - D_{25} + D_{26})M_H^2 + (D_0 + D_{11} - D_{13} - D_{25})s + (-D_{12} + D_{13} - D_{24} + D_{25})s_{12} + (-D_0 - D_{11} + D_{12} + D_{25} - D_{26})s_{23}]/v^3,$$

$$\mathscr{G}_5^\mu = 8m_t^2M_W^2[(3D_{11} + 2D_{24})q_1^\mu + (D_0 + 3D_{12} + 2D_{22})q_2^\mu + (D_0 + 2D_{12} + D_{13} + 2D_{26})q_3^\mu]/v^3,$$

TABLE III. Tree-level Higgs boson + b rate (fb), showing the individual contributions from the final states (3) $g + g \to b + \bar{b} + H$, (2) $g + b \to b + H$, and (-2) the splitting piece $g \to b + \bar{b} \otimes g + b \to b + H$. $\sigma_{\text{total}} = (3) + (2) - (-2)$ is the total tree-level rate to $O(\alpha_s^{(1,2)}G_F)$.

Tree-level Higgs boson + b rate (fb)							
M_H		Integrated cross section above p_T^{cut} (GeV)					
(GeV)		50	75	100	125	150	200
110	(3)	41.9	16.6	7.6	4.1	2.1	0.6
	(2)	46.4	18.0	8.0	3.9	2.1	0.7
	(-2)	42.7	16.8	7.7	3.9	2.1	0.7
	σ_{total}	45.6	17.8	8.2	4.1	2.1	0.6
140	(3)	25.6	11.4	5.7	2.9	1.8	0.5
	(2)	28.2	12.0	5.7	3.0	1.6	0.6
	(-2)	26.1	11.2	5.5	2.9	1.6	0.6
	σ_{total}	27.7	12.2	5.9	3.0	1.8	0.5
180	(3)	14.2	7.4	3.7	2.1	1.2	0.5
	(2)	15.6	7.2	3.7	2.1	1.2	0.5
	(-2)	14.5	6.7	3.5	2.0	1.2	0.5
	σ_{total}	15.3	7.9	3.9	2.2	1.2	0.5
400	(3)	1.4	0.8	0.5	0.3	0.2	0.1
	(2)	1.5	0.9	0.5	0.4	0.3	0.1
	(-2)	1.5	0.9	0.5	0.4	0.3	0.1
	σ_{total}	1.4	0.8	0.5	0.3	0.2	0.1

$$\mathcal{G}_6^\mu = 4m_t^4[(D_0+D_{11}+2D_{12}+2D_{24})q_1^\mu+(D_0+3D_{12}+2D_{22})q_2^\mu+(3D_{13}+2D_{26})q_3^\mu]/v^3,$$

$$\mathcal{G}_7^\mu = 8m_t^2M_W^2[(D_{11}+2D_{24})q_1^\mu+(D_{12}+2D_{22})q_2^\mu+(-D_0+2D_{12}-D_{13}+2D_{26})q_3^\mu]/v^3.$$

$$\mathcal{G}_8^\mu = 4m_t^4[(-D_0-D_{11}+2D_{12}+2D_{24})q_1^\mu+(D_{12}+2D_{22})q_2^\mu+(D_{13}+2D_{26})q_3^\mu]/v^3.$$

APPENDIX C: TREE-LEVEL $b(\bar{b})+H$ PRODUCTION

In Table I, we present the $O(\alpha_s G_F)$ tree-level rate for the associated production of a high-p_T Higgs boson and a bottom quark or antiquark. In this appendix, we show how to improve the tree-level calculation of the bH production rate to $O(\alpha_s^{(1,2)}G_F)$. The production rate for the associated production of a high-p_T Higgs boson and a bottom antiquark is the same as that for a high-p_T Higgs boson and a bottom quark, but it simplifies the discussion to separate the two processes.

The tree-level production rate of a high-p_T Higgs boson (with mass $\leqslant 400$ GeV) and a b quark at the LHC is dominated by three contributions: $g+b\to b+H$ [of $O(\alpha_s G_F)$], $g+g\to b+\bar{b}+H$, [of $O(\alpha_s^2 G_F)$], and a *subtracted* splitting piece, $g\to b+\bar{b}\otimes g+b\to b+H$ [of $O(\alpha_s^2 G_F)$]. The improved tree-level production rate $\sigma_{\rm total}$ to $O(\alpha_s^{(1,2)}G_F)$ is given by summing the contributions from the first two processes and subtracting the contribution from the third piece [14]. This *subtracted* term is needed to avoid double counting the contributions from the kinematic region where g and $\bar{b}$ are almost collinear in the three-body final state process $g+g\to b+\bar{b}+H$.

The *subtracted* splitting piece has the form

$$(\text{splitting piece}) = \int d\xi_1 d\xi_2 f_{g/A}(\xi_1,\mu)\widetilde{f_{b/B}}(\xi_2,\mu)\hat{\sigma}(g+b\to b+H) + \int d\xi_1 d\xi_2 f_{g/B}(\xi_2,\mu)\widetilde{f_{b/A}}(\xi_1,\mu)\hat{\sigma}(g+b\to b+H).$$

In this expression, $\hat{\sigma}$ is the constituent cross section, ξ_j is the momentum fraction carried by parton j, μ is the factorization scale which is chosen to be the same as the renormalization scale, $f_{j/A}(\xi,\mu)$ is the parton distribution function for parton j in hadron A, and $\widetilde{f_{j/A}}(\xi,\mu)$ is the effective parton density [in the modified minimal subtraction ($\overline{\rm MS}$) scheme] as defined by

$$\widetilde{f_{b(\bar{b})/A}}(\xi,\mu) = \frac{\alpha_s(\mu)}{2\pi}\ln\left(\frac{\mu^2}{m_b^2}\right)\int_\xi^1 \frac{dz}{z}\frac{z^2+(1-z)^2}{2} \times f_{g/A}\left(\frac{\xi}{z},\mu\right),$$

where $\alpha_s(\mu)$ is the strong coupling constant and m_b is the b-quark mass.

The individual and summed contributions of the processes to the total tree-level rate at the LHC are presented in Table III for several Higgs boson masses. (The $g+g\to b+\bar{b}+H$ rates are obtained from Pythia 5.7 [15].) To a good approximation, the total rate $\sigma_{\rm total}$, which is equal to $(3)+(2)-(-2)$, is given by the $g+g\to b+\bar{b}+H$ process, denoted as (3) in Table III. For very high p_T and an intermediate Higgs boson mass and for high p_T and a heavy Higgs boson mass, the $g+b\to b+H$ process, denoted as (2), and the splitting piece, denoted as (-2), cancel almost exactly. Another tree-level process $q+\bar{q}\to b+\bar{b}+H$ [of $O(\alpha_s^2 G_F)$] is three to four orders of magnitude smaller than $g+g\to b+\bar{b}+H$ and can be ignored.

[1] CDF Collaboration, F. Abe *et al.*, Phys. Rev. Lett. **73**, 225 (1994); D0 Collaboration, S. Abachi *et al.*, *ibid*. **72**, 2138 (1994).

[2] P. Darriulat, in *Proceedings of the 27th International Conference on High Energy Physics*, Glasgow, Scotland, 1994, edited by P. J. Bussey and I. G. Knowles (IOP, London, 1995).

[3] J.F. Gunion, H.E. Haber, G.L. Kane, and S. Dawson, *The Higgs Hunter's Guide* (Addison-Wesley, Reading, MA, 1990).

[4] P. Giacomelli, 2nd Trieste Conference on Recent Development in the Phenomenology of Particle Physics, Report No. CERN-PPE-93-18, 1993 (unpublished).

[5] A. Stange, W. Marciano, and S. Willenbrock, Phys. Rev. D **49**, 1354 (1994); J.F. Gunion and T. Han, *ibid*. **51**, 1051 (1995); S. Mrenna and G.L. Kane, Report No. hep-ph/9406337, 1994 (unpublished).

[6] R. Arnowitt and P. Nath, Phys. Rev. Lett. **70**, 3696 (1993); J.L. Lopez, D.V. Nanopoulos, H. Pois, X. Wang, and A. Zichichi, Phys. Lett. B **306**, 73 (1993); G.L. Kane, C. Kolda, L. Roszkowski, and J.D. Wells, Phys. Rev. D **49**, 6173 (1994).

[7] G.L. Kane, C. Kolda, and J.D. Wells, Phys. Rev. Lett. **70**, 2686 (1993).

[8] R. Chivukula, M. Dugan, and M. Golden, Phys. Lett. B **336**, 62 (1994).

[9] R.K. Ellis, I. Hinchliffe, M. Soldate, and J.J. van der Bij, Nucl. Phys. **B297**, 221 (1988).

[10] S. Dawson and R.P. Kauffman, Phys. Rev. Lett. **68**, 2273 (1992).

[11] G.J. van Oldenborgh, ''FF, A Package to Evaluate One-Loop Feynman Diagrams,'' Report No. NIKHEF-H/90-15, 1990 (unpublished).

[12] J. Botts, J. Huston, H. Lai, J. Morfin, J. Owens, J. Qiu, W.-K. Tung, H. Weerts, Michigan State University Report No. MSUTH-93/17 (unpublished).

[13] E. Malkawi and C.-P. Yuan, Phys. Rev. D **50**, 4462 (1994); C.-P. Yuan, *VIth Mexican School of Particles and Fields*, Proceedings, Villahermosa, Mexico, 1994 (World Scientific, Singapore, 1995).

[14] J.C. Collins and W.-K. Tung, Nucl. Phys. **B278**, 934 (1986); D.A. Dicus and S. Willenbrock, Phys. Rev. D **39**, 751 (1989); D.O. Carlson, Ph.D. thesis, Michigan State University, 1995; D.O. Carlson and C.-P. Yuan, Report No. MSUHEP-50823, 1995 (unpublished).

[15] H.U. Bengtsson and T. Sjostrand, Comput. Phys. Commun. **43**, 43 (1987).